

# Creation of Bioorthogonal Redox Systems Depending on Nicotinamide Flucytosine Dinucleotide

Debin Ji,<sup>†,‡</sup> Lei Wang,<sup>†,‡</sup> Shuhua Hou,<sup>†,‡</sup> Wujun Liu,<sup>†,§</sup> Jinxia Wang,<sup>†</sup> Qian Wang,<sup>†,§</sup> and Zongbao K. Zhao<sup>\*,†,§</sup>

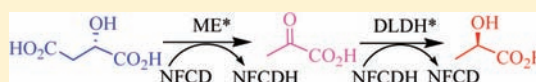
<sup>†</sup>Dalian Institute of Chemical Physics, Chinese Academy of Sciences, Dalian 116023, China

<sup>‡</sup>Graduate University of Chinese Academy of Sciences, Beijing 100039, China

<sup>§</sup>Dalian National Laboratory for Clean Energy, Dalian 116023, China

## Supporting Information

**ABSTRACT:** Many enzymes catalyzing biological redox chemistry depend on the omnipresent cofactor, nicotinamide adenine dinucleotide (NAD). NAD is also involved in various nonredox processes. It remains challenging to disconnect one particular NAD-dependent reaction from all others. Here we present a bioorthogonal system that catalyzes the oxidative decarboxylation of L-malate with a dedicated abiotic cofactor, nicotinamide flucytosine dinucleotide (NFCD). By screening the multisite saturated mutagenesis libraries of the NAD-dependent malic enzyme (ME), we identified the mutant ME-L310R/Q401C, which showed excellent activity with NFCD, yet marginal activity with NAD. We found that another synthetic cofactor, nicotinamide cytosine dinucleotide (NCD), also displayed similar activity with the ME mutants. Inspired by these observations, we mutated D-lactate dehydrogenase (DLDH) and malate dehydrogenase (MDH) to DLDH-V152R and MDH-L6R, respectively, and both mutants showed fully active with NFCD. When coupled with DLDH-V152R, ME-L310R/Q401C required only a catalytic amount of NFCD to convert L-malate. Our results opened the window to engineer bioorthogonal redox systems for a wide variety of applications in systems biology and synthetic biology.



## INTRODUCTION

Biological redox chemistry is catalyzed by numerous enzymes that depend only on a few cofactors.<sup>1</sup> One of the most important cofactors is nicotinamide adenine dinucleotide (NAD, Figure 1).<sup>2</sup> NAD is also involved in protein post-

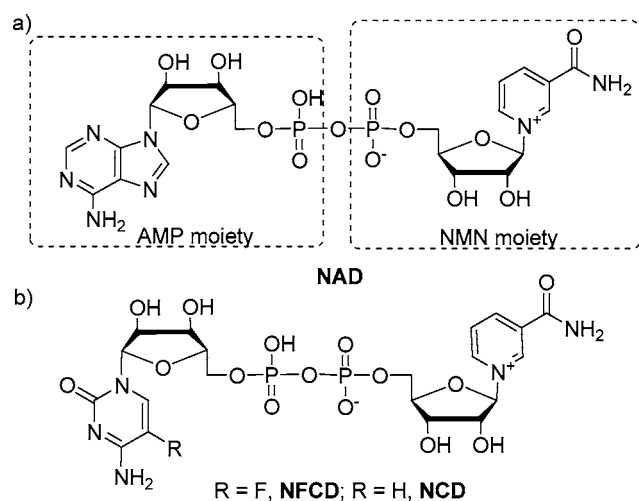


**Figure 1.** Chemical structures of NAD, NFCD, and NCD.

translational modification and signal transduction, thus mediating calcium homeostasis, gene expression, carcinogenesis, aging, and cell death.<sup>3</sup> Because so many cellular

processes are connected to NAD, any perturbations lead to NAD concentration fluctuation should have major global effects.<sup>4</sup> In order to manipulate a specific NAD-dependent redox reaction, genetic tools, such as gene knockout, promoter engineering, and similar techniques,<sup>5</sup> are currently at our disposal. While genetic tools are focused on controlling the concentration of the targeted protein, a conceptually novel approach that employs non-natural cofactor for the redox chemistry, to the best of our knowledge, remains to be demonstrated.

We believe that the biological redox chemistry can be controlled if the corresponding enzyme is engineered to respond specifically and efficiently to an abiotic cofactor, thus disconnecting the reaction-of-interest from other NAD-dependent events. In other words, such an engineered enzyme/cofactor combination holds an identical biochemistry yet distinguishes itself as a bioorthogonal system.<sup>6</sup> Such a system is particularly useful as a tool in synthetic biology to generate a pathway-specific driving force. It can also be applied to analyze the metabolic network for systems biology. Although changing cofactor specificity of oxidoreductases has been pursued over the years, previous studies have been reversing the preference between two natural cofactors, NAD and its phosphorylated form, NADP.<sup>7</sup> In sharp contrast to other examples in lowering enzymatic activity through inhibition by small molecules,<sup>8</sup> the

Received: August 6, 2011

Published: November 19, 2011

key for a cofactor-dependent bioorthogonal redox system is to maintain the original activity in terms of substrate recognition and catalytic efficiency. Here we present the creation of bioorthogonal systems that catalyze the oxidative decarboxylation of L-malate with abiotic cofactors, nicotinamide flucytosine dinucleotide (NFCD), or nicotinamide cytosine dinucleotide (NCD, Figure 1). We show that mutants of D-lactate dehydrogenase (DLDH) and malate dehydrogenase (MDH) can also be engineered to favor NFCD over NAD. Our results opened the window to engineer bioorthogonal redox systems for a wide variety of applications in systems biology and synthetic biology.

## RESULTS AND DISCUSSION

**Designing the Abiotic Cofactor.** The chemical structure of NAD consists of the adenosine monophosphate moiety (AMP) and the nicotinamide mononucleotide moiety (NMN). While AMP is largely responsible for recognizing and binding the cofactor to the receptor, NMN is essential to mediate the redox chemistry. To ensure its proper function as a cofactor capable of matching the structural and functional space of the elusive protein,<sup>9</sup> an NAD analog should have at least two structural features: an intact NMN moiety and a novel structure to substitute the AMP part. However, further decorating of the adenine core according to the established “bump-and-hole” strategy used in kinase study<sup>10</sup> is not preferred, because a mutant enzyme that binds such NAD analogs will most likely bind NAD with substantial affinity. As a result, NAD will have a significant contribution to the reaction-of-interest if the enzyme is incorporated in a cell, that is to say, the system is not bioorthogonal.

Here we replaced the adenine moiety by a non-natural pyrimidine base, flucytosine, leading to the NAD analog, NFCD. The synthesis of NFCD was realized by coupling NMN with 5-fluorocytidine monophosphate in a 45% isolated yield according to the literature procedures.<sup>11</sup> Choosing NFCD in this study was based on two considerations: First, structural differences between adenine and flucytosine are remarkable in terms of molecule volume and hydrogen-bonding capacity. Molecular interactions involving NFCD are expected to be substantially different from those of NAD, providing the possibility to realize bioorthogonal protein–ligand binding patterns. It should be noted that the creation of orthogonal ligand for mutant human estrogen receptors using similar strategy has been previously demonstrated.<sup>12</sup> Second, the F atom in NFCD could be detected by <sup>19</sup>F NMR, which is potentially useful to trace this cofactor in the reaction system.

**Constructing Mutant Libraries of ME.** Malic enzyme (ME) catalyzes an oxidative decarboxylation of L-malate to give pyruvate with concomitant reduction of NAD to NADH.<sup>13</sup> There are 19 eukaryotic MEs with their crystal structures accessible in the Protein Data Bank. These MEs have similar overall tertiary structure albeit with small local differences. We selected the *Escherichia coli* (*E. coli*) NAD-dependent ME (NCBI no. NP\_415996.1) as our model redox enzyme, largely because there should be less technical risk for the protein expression and the screening experiments using *E. coli* as the host. As the crystal structure of the *E. coli* ME remains unavailable, we generated a structure model for this enzyme using SWISS-MODEL.<sup>14</sup> We chose 1LLQ (ME from *Ascaris suum*) as the template because the sequence identity of the *E. coli* ME with 1LLQ was 41%. The adenine binding pocket of this enzyme was identified (Figure 2), and three residues, L310,

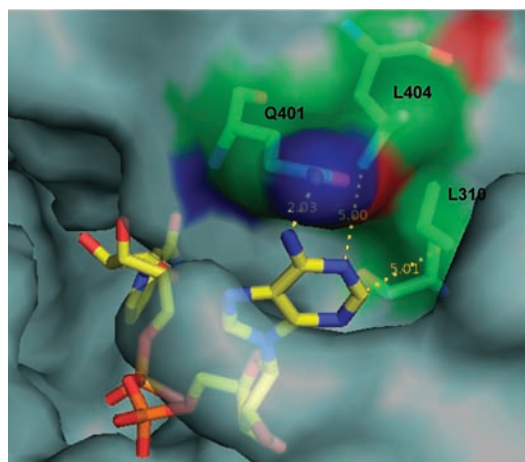


**Figure 2.** Surface view of the ME model binding with NAD. The residues depicted as sticks were chosen to mutate in our experiment.

Q401, and L404 were selected for mutagenesis, as they were in close proximity to the adenine moiety in the structure model. The distances of L310, Q401, and L404 to the adenine moiety are 5.01, 2.03, and 5.00 Å, respectively.

Although a single expression library of ME with saturate mutagenesis on all these three sites can be produced in principle according to the literature method,<sup>15</sup> we realized that, to reach 95% probability of mutant coverage in that library, over  $1 \times 10^5$  clones have to be screened,<sup>16</sup> an incredible task for an academic laboratory. To make the library practical for screening, we constructed three two-site-saturated mutagenesis libraries, L310/Q401, L310/L404, and Q401/L404, using a polymerase chain reaction (PCR)-based strategy with the plasmid pET24b-ME.<sup>15</sup> A few clones from each library were cultured in Luria–Bertani (LB) liquid media and induced by isopropyl  $\beta$ -D-1-thiogalactopyranoside (IPTG). Crude cell lysate of those clones was analyzed by polyacrylamide gel electrophoresis. Results showed that most clones had a strong protein band around 65 kDa (data not shown), indicating that these libraries were qualified for screening.

**Screening of Mutant Libraries.** We screened these libraries by using a coupled assay that recycles the cofactor and develops a blue color.<sup>17</sup> For the library Q401/L404, we failed to identify a clone that had strong cofactor preference over NFCD. Over 50% clones had reduced but had considerable activity with NAD, and mutants that had noticeable activity with NFCD showed similar or higher activity with NAD. However, 14 and 6 clones were identified from the library L310/Q401 and L310/L404, respectively, about 470 and 300 clones were screened. These clones showed significant higher activity with NFCD than NAD. Sequencing analysis of these clones revealed that mutations at the sites Q401 and L404 appeared with little convergence except the absence of aromatic amino acid residues (Table 1). However, mutations at the L310 site were strictly conserved, as 18 and 2 out of the 20 clones had L310R and L310K, respectively. The single mutant, ME-L310R, was also obtained from the library L310/L404. Arginine (R) and lysine (K) are basic amino acids with long side chains. The replacement of leucine (L) with R or K around the adenine binding pocket may reduce the volume of the pocket and offer additional hydrogen-bonding opportunities, leading to a better fit for NFCD. Specifically, new hydrogen bonding may be established between the S-

**Table 1. Screening Results and the Specific Activity of ME Mutants with NAD and NFCD<sup>a</sup>**

ME mutation	no. of clones	NAD (U/mg)	NFCD (U/mg)
L310R	1	3.7 ± 0.5	10.9 ± 0.7
L310R, L404T	1	7.9 ± 0.4	1.6 ± 0.3
L310R, L404N	1	4.6 ± 0.2	3.4 ± 0.2
L310R, L404C	1	2.5 ± 0.1	4.0 ± 0.3
L310R, L404I	1	2.0 ± 0.1	3.2 ± 0.1
L310K, L404S	1	16.8 ± 1.1	7.1 ± 0.5
L310R, Q401S	2	2.9 ± 0.1	11.5 ± 0.6
L310R, Q401N	4	3.2 ± 0.2	5.2 ± 0.4
L310R, Q401I	2	1.9 ± 0.3	3.2 ± 0.2
L310R, Q401C	1	3.1 ± 0.1	13.2 ± 0.6
L310R, Q401V	1	3.2 ± 0.1	10.1 ± 0.5
L310R, Q401D	2	1.6 ± 0.2	2.7 ± 0.2
L310R, Q401G	1	1.1 ± 0.0	1.3 ± 0.0
L310K, Q401G	1	5.9 ± 0.2	12.6 ± 0.3

<sup>a</sup>The specific activity was determined, while the concentration of NAD and NFCD was at 2 and 0.2 mM, respectively.

fluorocytidine moiety and the basic amino acid side chains. We further purified all of these mutants to near homogeneity and assayed their specific activity with NFCD and NAD (Table 1). Results confirmed our observations that they were all active with NFCD. Compared with the ME-L310R mutant, most proteins bearing an additional mutation at either the L404 or the Q401 site had a reduced cofactor preference over NFCD; one particular mutant, ME-L310R/Q401C, showed an increased NFCD preference.

**Kinetic Analysis.** The kinetic parameters of ME, ME-L310R, and ME-L310R/Q401C using both NAD and NFCD as the cofactors were assayed (Table 2). The catalytic efficiency ( $k_{\text{cat}}/K_{\text{m}}$ ) of ME with NFCD was only 0.93% of that with NAD, clearly indicating that the wild-type protein preferred NAD. For ME-L310R and ME-L310R/Q401C, in contrast, the  $k_{\text{cat}}/K_{\text{m}}$  values with NAD were only 1.0% and 0.37%, respectively, of that with NFCD, suggesting that these mutants strongly preferred NFCD. For the mutant ME-L310R/Q401C, the  $k_{\text{cat}}/K_{\text{mNFCD}}$  value was 48.3-fold higher than that of ME, while the  $k_{\text{cat}}/K_{\text{mNAD}}$  value was only 0.16% of that of ME. Thus, compared with ME catalysis using NAD as the cofactor, ME-L310R/Q401C achieved an approximately 30 000-fold cofactor specificity shift toward NFCD. The  $K_{\text{mNFCD}}$  value for ME-L310R/Q401C was 6.3-fold higher than  $K_{\text{mNAD}}$  for ME, indicating that the binding affinity between NFCD and ME-L310R/Q401C was weaker than that between NAD and ME. However, the  $k_{\text{catNFCD}}$  values for ME-L310R and ME-L310R/Q401C were higher than  $k_{\text{catNAD}}$  for ME, indicating that these mutant enzymes turned over the substrate more rapidly in the natural system. Overall, the catalytic efficiency of ME-L310R/Q401C with NFCD was comparable to that of ME with NAD,

suggesting that the engineered redox system attained similar catalytic power to the natural one.

**Activity of NCD.** After the successful demonstration of NFCD as an abiotic redox cofactor, we decided to test whether NCD could also be recognized by these ME mutants. NCD can be envisioned as the defluorinated version of NFCD. Because NCD is the coupling product of cytidine monophosphate and NMN, both of which are naturally occurring metabolites, the creation of NCD-dependent enzymes may provide an opportunity to better understand the history of redox cofactor evolution.<sup>18</sup> We prepared NCD in 11% isolated yield, according to the literature procedures,<sup>11</sup> and found these ME mutants were also active in the presence of NCD. Detailed kinetic parameters of ME, ME-L310R, and ME-L310R/Q401C using NCD as the cofactor are shown in Table 2. Again, the  $k_{\text{catNCD}}$  values for ME-L310R and ME-L310R/Q401C were higher than  $k_{\text{catNAD}}$  for ME, indicating that these mutant enzymes turned over the substrate more rapidly using NCD as the cofactor than ME did using NAD as the cofactor. It was clear that both ME-L310R and ME-L310R/Q401C had lower  $K_{\text{m}}$  values for NCD than those for NFCD. Because of this, catalytic efficiencies with NCD were significantly improved in comparison to those with NFCD. The fact that  $K_{\text{mNCD}}$  was lower than  $K_{\text{mNFCD}}$  suggested that, the presence of the strong electron-withdrawing group F at the C<sup>5</sup> position of cytidine facilitated a weaker molecular interaction between the ligand and the proteins.

**Exploring Other Oxidoreductases.** It occurred to us that the L310 residue is located immediately at the N-terminus of the conserved GX(X)GXXG sequence in Rossmann fold motif<sup>19</sup> of ME. The protein cofactor interactions are largely conserved in NAD-dependent enzymes.<sup>20</sup> We thus collected a number of oxidoreductases and compared their amino acid sequences (Figure 3a). It is evident that the position corresponding to L310 of ME is taken by a L, I, or V residue. A common feature of these residues is that they all have an alkyl hydrophobic side chain. We checked the distances of these residues from the adenine group in these proteins and found that the distance of that residue from the adenine group is in the range of 3.70–5.56 Å (Table S1, Supporting Information). Because our early screening experiment observed a number of active ME mutants bearing an R mutation at this position, we imagined that changing this particular residue to R in other NAD-dependent oxidoreductases may also lead to active mutants that take NFCD as the cofactor.

One particular enzyme included in the above sequence comparison is D-lactate dehydrogenase (DLDH, PDB id 2DLD) from *Lactobacillus helveticus*.<sup>21</sup> DLDH catalyzes the interconversion of D-lactate and pyruvate with a concomitant interconversion of NAD and NADH. We selected this enzyme to test our speculation, because if successful, we should be able to develop a coupled system to regenerate NFCD. As V152 in DLDH is the counterpart of L310 in ME, we overproduced DLDH and the mutant DLDH-V152R in *E. coli*. As expected, in

**Table 2. Kinetic Parameters for ME and Its Mutants Using NAD, NFCD, and NCD As Cofactors**

enzyme	NAD			NFCD			NCD		
	$K_{\text{m}}$ (mM)	$k_{\text{cat}}$ (s <sup>-1</sup> )	$k_{\text{cat}}/K_{\text{m}}$ (mM <sup>-1</sup> s <sup>-1</sup> )	$K_{\text{m}}$ (mM)	$k_{\text{cat}}$ (s <sup>-1</sup> )	$k_{\text{cat}}/K_{\text{m}}$ (mM <sup>-1</sup> s <sup>-1</sup> )	$K_{\text{m}}$ (mM)	$k_{\text{cat}}$ (s <sup>-1</sup> )	$k_{\text{cat}}/K_{\text{m}}$ (mM <sup>-1</sup> s <sup>-1</sup> )
ME	0.27 ± 0.01	57.3 ± 0.4	214.8	11.9 ± 0.8	23.6 ± 1.2	2.0	9.4 ± 1.9	26.1 ± 4.1	2.8
ME-L310R	5.6 ± 1.1	5.0 ± 0.8	0.90	1.2 ± 0.3	105.3 ± 16.7	88.4	0.60 ± 0.10	102.0 ± 8.6	169.9
ME-L310R/Q401C	10.4 ± 1.2	3.8 ± 0.4	0.36	1.7 ± 0.2	162.4 ± 17.2	96.7	1.02 ± 0.17	158.2 ± 17.8	154.6



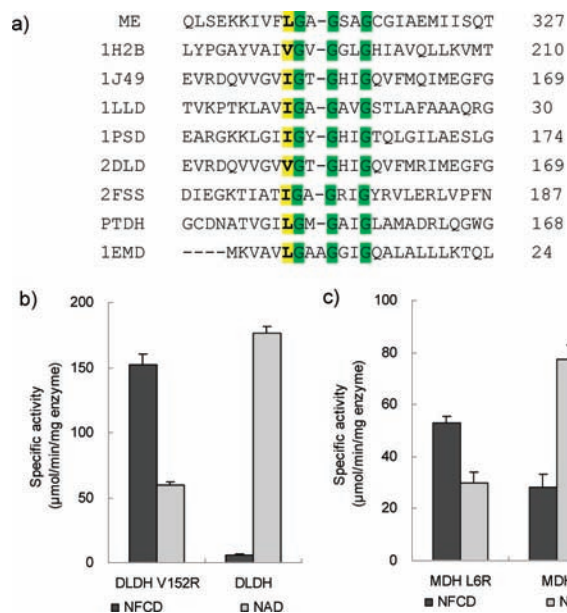


**Figure 3.** System transfer to other dehydrogenases. (a) Sequence alignment of ME with other dehydrogenases, including alcohol dehydrogenase (1H2B), D-LDH (1J49 and 2DL2), L-LDH (1LLD), D-3-phosphoglycerate dehydrogenase (1PSD), formate dehydrogenase (2FSS), phosphite dehydrogenase (PTDH), MDH (1EMD). Residues in green represent the identity sequence of GX(X)GXXG nucleotide binding motif. Residues in yellow represent the similarity sequence. (b) The specific activity of DLDH and DLDH-V152R with NAD and NFCD, respectively. (c) The specific activity of MDH and MDH-L6R with NAD and NFCD, respectively.

the presence of NFCD, DLDH was barely active, but DLDH-V152R was active with an estimated specific activity of  $152.0 \pm 8.8$  U  $\text{mg}^{-1}$  (Figure 3b). It was noticeable that the specific activity of DLDH with NAD was  $176.3 \pm 5.3$  U  $\text{mg}^{-1}$  under identical assay conditions. Thus, by changing one conserved amino acid residue, we attained the mutant DLDH-V152R that catalyzed the oxidation of D-lactate to pyruvate in the presence of NFCD at a comparable efficiency to that of the natural system with DLDH and NAD.

MDH (PDB id 1EMD) from *E. coli* was also selected to test our speculation.<sup>22</sup> MDH catalyzes the oxidation of malate to oxaloacetate with a concomitant reduction of NAD to NADH. The conserved glycine-rich sequence pattern in MDH is GXXGXXG instead of GXGXXG. The distance of 5.56 Å from the adenine moiety to L6, the counterpart of L310 in ME, is about 1.1-fold longer than that of the ME case. We overproduced MDH and the mutant MDH-L6R. Again, results showed that MDH-L6R favored NFCD over NAD and that it had reduced activity with NAD (Figure 3c).

Although our rationally designed mutants DLDH-V152R and MDH-L6R both reserved appreciable activity in the presence of NAD, other variants are expected to concurrently achieve reduced activity with NAD and improved activity with NFCD should additional mutations be introduced, as for ME. We also think that, except for those NAD-dependent oxidoreductases without conventional Rossmann fold structure,<sup>23</sup> many more enzymes should be manageable similarly to generate new mutants to recognize NFCD specifically. However, it should be cautioned that mutations close to the conserved Rossmann fold sequence may also lead to impaired protein folding, thus

presenting more difficulties to find alternative sites for mutagenesis.

**Regeneration of NFCD.** With ME-L310R/Q401C and DLDH-V152R in hand, we were able to demonstrate the regeneration of NFCD in vitro. In this system, L-malate was first oxidized to pyruvate by the former enzyme with a reduction of NFCD to NFCDH, and then pyruvate was reduced to lactate by the latter enzyme with an oxidation of NFCDH to NFCD (Figure 4a). In a typical experiment, L-

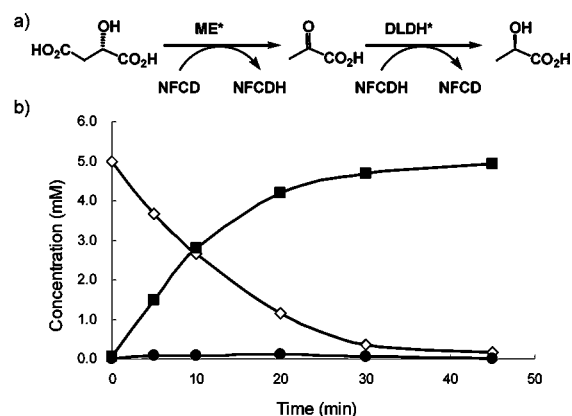


**Figure 4.** (a) Cofactor recycling system of NFCD with ME\* (ME-L310R/Q401C) and DLDH\* (DLDH-V152R). (b) The progress of the reaction was monitored by ion chromatography. Lactate (□), pyruvate (●), and L-malate (◇).

malate (5 mM) was almost completely converted into lactate in the presence of NFCD (0.2 mM) in 45 min (Figure 4 b), indicating that NFCD was recycled at least 24 times. For the first 20 min, the system turned over 0.2 mM L-malate per min. It should be emphasized that the coupled system of ME-L310R/Q401C and DLDH-V152R in the presence of NFCD produced D-lactate exclusively (Supporting Information). Similarly, we also noticed that both ME-L310R and ME-L310R/Q401C took L-malate, not D-malate, as their substrate when NFCD was used as the cofactor. These results indicated that mutations in the adenine binding pocket of NAD-dependent oxidoreductases did not lead to a compromise in stereoselectivity in terms of substrate recognition or product formation. The recyclability of NFCD and the stringent stereoselectivity of these examples suggested that NFCD can potentially be applied in vivo to drive or control a naturally NAD-dependent reaction, independent of the cellular NAD level.

## CONCLUSIONS

We have demonstrated that, by matching abiotic cofactors and semirationally designed ME mutants, bioorthogonal redox system can be established. We showed that the strategy was potentially applicable for other NAD-dependent oxidoreductases. In the future, we hope to further expand the scope of this strategy and apply those bioorthogonal redox systems in vivo. It should be noted that a number of transporters for NAD and similar compounds have been available.<sup>24</sup> In particular, we recently showed that the nucleotide transporter NTT4 from the chlamydial endosymbiont *Protochlamydia amoebophila* UWE25, can confer *E. coli* cells to take NAD from the culture broth and that engineered *E. coli* strains incapable of making NAD intracellularly can grow well when NAD is fed in the

culture broth.<sup>25</sup> Therefore, to deliver synthetic NAD analogs should be manageable. Nonspecific interactions between the synthetic cofactor and other cellular components are among the other concerns to be addressed. Nonetheless, the accessibility of such bioorthogonal redox systems should provide unique tools for synthetic biology to assemble pathway-specific redox chemistry and for systems biology to elucidate the contributions of individual redox steps in the metabolic network.

## EXPERIMENTAL PROCEDURES

All reagents and starting materials were used as obtained from commercial suppliers (Sigma, ABCR, ACROS) unless otherwise indicated. Commercial nucleotides were phosphorylated as previously reported to give the corresponding monophosphates.<sup>26</sup> NMN was prepared by hydrolysis of NAD as reported.<sup>27</sup>

**Synthesis of NFCD and NCD.** A reaction mixture containing NMN (150 mg, 0.45 mM),  $\text{Ph}_3\text{P}$  (0.396 g, 1.5 mM),  $(\text{PyS})_2$  (0.33 g, 1.5 mM), and *L*-methylimidazole (0.48 mL, 6 mM) in DMF/DMSO (1:2, 10 mL) was held at room temperature for 15 min. A solution of 5-fluorocytidine monophosphate (0.9 mM) in 2 mL DMF was added. The mixture was stirred at room temperature for 50 min. To the mixture was added acetone (100 mL). The precipitates were collected and washed twice with acetone. Purification of the product was performed by anion exchange column chromatography using 201 × 4 type anion resin ( $\text{HCO}_2^-$  form) and eluted with 50 mM  $\text{HCO}_2\text{H}$ . Fractions containing the product were concentrated and further purified on a DEAE Sephadex G-25 column using 10 mM  $\text{NH}_4\text{HCO}_3$  as the elution buffer. Fractions were pooled, lyophilized, dissolved in water, and lyophilized to give NFCD as a white solid (145 mg, yield 45%).  $^1\text{H}$  NMR ( $\text{D}_2\text{O}$ , 400 MHz,  $\text{NH}_4^+$  form):  $\delta$  9.17 (s, 1H), 9.02 (d,  $J = 6.1$  Hz, 1H), 8.72 (d,  $J = 7.9$  Hz, 1H), 8.05 (m, 1H), 7.70 (d,  $J = 6.4$  Hz, 1H), 5.94 (d,  $J = 5.5$  Hz, 1H), 5.55 (d,  $J = 3.8$  Hz, 1H), 4.33 (brs, 1H), 4.28 (brs, 1H), 4.19 (brs, 1H), 4.15–4.12 (m, 1H), 4.03–3.93 (m, 5H), 3.91–3.89 (m, 1H).  $^{13}\text{C}$  NMR ( $\text{D}_2\text{O}$ , 100 MHz,  $\text{NH}_4^+$  form):  $\delta$  165.2, 158.0, 157.8, 155.3, 145.9, 142.4, 139.8, 138.5, 136.0, 133.7, 128.6, 125.5, 125.2, 99.8, 89.5, 86.6, 82.3, 77.4, 74.0, 70.3, 69.0, 64.8, 64.7.  $^{19}\text{F}$  NMR ( $\text{D}_2\text{O}$ , 376 MHz,  $\text{NH}_4^+$  form):  $\delta$  -164.9.  $^{31}\text{P}$  NMR ( $\text{D}_2\text{O}$ , 162 MHz,  $\text{NH}_4^+$  form):  $\delta$  -11.1, -11.2. HRMS: calculated for  $\text{C}_{20}\text{H}_{26}\text{FN}_5\text{O}_{15}\text{P}_2$  ( $\text{M} + \text{H}^+$ )<sup>+</sup> 658.0963; found 658.0961.

NCD (38 mg, 11%) as a white powder was prepared similarly.  $^1\text{H}$  NMR ( $\text{D}_2\text{O}$ , 400 MHz,  $\text{NH}_4^+$  form):  $\delta$  9.30 (s, 1H), 9.14 (d,  $J = 6.1$  Hz, 1H), 8.83 (d,  $J = 7.9$  Hz, 1H), 8.16 (m, 1H), 7.74 (d,  $J = 7.6$  Hz, 1H), 6.04 (d,  $J = 5.3$  Hz, 1H), 5.92 (d,  $J = 7.4$  Hz, 1H), 5.77 (d,  $J = 4.0$  Hz, 1H), 4.46 (brs, 1H), 4.41 (brs, 1H), 4.33 (brs, 1H), 4.28–4.25 (m, 1H), 4.17–4.09 (m, 5H), 4.02–4.00 (m, 1H).  $^{13}\text{C}$  NMR ( $\text{D}_2\text{O}$ , 100 MHz,  $\text{NH}_4^+$  form):  $\delta$  165.5, 165.2, 156.4, 146.0, 142.5, 141.7, 139.9, 133.9, 128.6, 99.9, 89.4, 87.0, 82.5, 77.6, 74.1, 70.7, 69.2, 64.9, 64.7.  $^{31}\text{P}$  NMR ( $\text{D}_2\text{O}$ , 162 MHz,  $\text{NH}_4^+$  form):  $\delta$  -11.1, -11.3. HRMS: calculated for  $\text{C}_{20}\text{H}_{27}\text{N}_5\text{O}_{15}\text{P}_2$  ( $\text{M} + \text{Na}^+$ )<sup>+</sup> 662.0877; found 662.0883.

**Construction of Mutant Libraries.** Two-site saturation mutant libraries were constructed according to previous methods.<sup>15</sup> To construct the libraries Q401/L404, L310/Q401, and L310/L404, degenerated primer ( $\text{K} = \text{G}$  or  $\text{T}$ ;  $\text{M} = \text{C}$  or  $\text{A}$ ;  $\text{N} = \text{A}$ ,  $\text{C}$ ,  $\text{G}$ , or  $\text{T}$ ) pairs 5'-GTCTCAGGANNKACCGGGNNKTTTACGGAAGAGATCATCCG-3' and 5'-TTCCGTAAAMNNCCCGGTMNNTCCTGAGCAGCCAATCAG-3', 5'-ATCGTCTTCNN KGGTGCAGGTTGAGC-3' and 5'-ACAGCCCGGTMNNT CCTGAGCAGCCAATCAGAAATATC-3', and 5'-ATCGTCTT CANNKGGTGCAGGTT-C A G C - 3' and 5'-T C T T C C G T A A A M NNCCCGGTTCTGCTGAGAC-3', respectively, were used. Fragments containing mutagenic modifications were obtained by PCR using the corresponding primer pairs and the plasmid pET24b-ME as the template. The resulted DNA fragments were used as megaprimer to amplify the plasmid pET24b-ME to generate nicked plasmid DNA containing the corresponding mutations. The PCR mixtures were treated with DpnI (New England Biolabs, Beijing, China) to digest the methylated parental plasmid and transformed into electrocompetent *E. coli* BL21 (DE3) cells to get the expression libraries.

**High-Throughput Screening of ME Variants.**<sup>17</sup> Recombinant *E. coli* colonies from the libraries were grown on LB agar plates containing 0.5 mM of IPTG and 50  $\mu\text{g mL}^{-1}$  of kanamycin. After incubated at 30 °C for 36 h, the colonies were picked to a 96-well plate. Cells were resuspended in 100  $\mu\text{L}$  of lysis buffer (50 mM of HEPES, 1 mg  $\text{mL}^{-1}$  of lysozyme, 1% Triton X100, and pH of 7.5) and lysed by shaking at 37 °C for 1 h. Samples were centrifugation at 4000 g for 15 min, and supernatants were collected and stored at 4 °C. Assays were performed by transferring 10  $\mu\text{L}$  of each supernatant to 90  $\mu\text{L}$  of reaction buffer (50 mM of HEPES, 3 mM of *L*-malate, 5 mM of  $\text{MnCl}_2$ , 0.05 mM of NAD or NFCD, 0.1 mM of nitro blue tetrazolium, 0.025 mM of phenazine methosulfate, and pH of 7.2). After being incubated at 37 °C for 5 min, the plates were monitored at 580 nm on a PowerWave XS universal microplate spectrophotometer (Bio-Tek instruments Inc., Vermont). For library screening, each 96-well plate contained a positive control using ME and a negative control with no enzyme. The positive clones were picked from the corresponding spots on the agar plate.

### Activity and Kinetic Assay of ME and Its Variants.

Overexpression and purification of recombinant MEs were performed as previously described.<sup>28</sup> The activity assays were carried out at 25 °C in 1 cm cuvettes using UV-vis spectrophotometer model V-53 (JASCO, Tokyo, Japan). The activity was measured in 50 mM of HEPES and pH of 7.2 and in the presence of 3 mM of *L*-malate and 5 mM of  $\text{MnCl}_2$  at varying concentrations of NAD or NFCD. After adding the enzyme solution into the reaction mixture, the absorbance at 340 nm was continuously monitored for 1 min. One enzyme unit is defined as the amount of enzyme that catalyzes the formation of 1  $\mu\text{M}$  of NADH or NFCDH per minute under the assay conditions. A molar absorption coefficient of 6220  $\text{M}^{-1} \text{cm}^{-1}$  for NADH, NFCDH, or NCDH was used in the calculations.

For kinetic assay, the Michaelis–Menten constants  $V_{\text{max}}$  and  $K_{\text{m}}$  of NAD, NFCD, and NCD of the wild-type and mutant ME were obtained from initial rate measurements under conditions in which coenzyme was varied at five different levels from below their  $K_{\text{m}}$  to above their  $K_{\text{m}}$ . The *L*-malate (5 mM) and  $\text{Mn}^{2+}$  (5 mM) were present at a saturated and constant concentration. The experimental data were fitted with the Michaelis–Menten equation using OriginLab 8.0. Reactions were incubated in 50 mM of HEPES and pH of 7.5 at 25 °C. All assays were performed in duplicates.

### Constructing DLDH and MDH Expression Plasmid and Mutagenesis.

The gene of DLDH (GenBank No. CAA47255.1) from *L. helveticus* was synthesized and inserted between *Nde*I and *Xho*I in the pET24b vector (Novagen) with a C-terminal Leu-Glu as a spacer between the protein and the His<sub>6</sub> tag. The gene of MDH (GenBank no. CAA68326.1) was isolated from the *E. coli* genome and inserted similarly, as was done for DLDH. The mutants DLDH-V152R and MDH L6R were created by a method as described in the QuikChange site-directed mutagenesis kit (Invitrogen).

### Activity Assay of DLDH, MDH, and Their Mutants.

The specific activity of DLDH was measured at 25 °C in 1 cm cuvettes using the UV-vis spectrophotometer. The activity assays were performed in a total volume of 0.2 mL. The reaction buffer contained 50 mM of HEPES, pH of 7.5, 200 mM of D-lactate, and 1 mM of NFCD or NAD. After adding 1  $\mu\text{L}$  of DLDH solution (0.1 mg  $\text{mL}^{-1}$ ) into the reaction mixture, the absorbance at 340 nm was continuously monitored for 1 min, and data were processed as described.

The specific activity of MDH was measured, as was done for DLDH. The reaction buffer contained 50 mM of Tris-HCl, pH of 8.0, 100 mM of *L*-malate, and 1 mM of NFCD or NAD.

**Cofactor Recycling.** The cofactor recycling experiment with ME-L310R/Q401C and DLDH-V152R was performed in 50 mM of HEPES and pH of 7.5, which contained 5 mM of *L*-malate, 2.5 mM of  $\text{MnCl}_2$ , 0.2 mM of NFCD, 0.002 mg  $\text{mL}^{-1}$  of DLDH-V152R, and 0.008 mg  $\text{mL}^{-1}$  of ME-L310R/Q401C. The reaction mixtures were incubated at 25 °C for 45 min. The concentrations of lactate, pyruvate, and malate were determined by ICS-2500 ion chromatography system (Dionex, Sunnyvale, California), equipped with a guard column IonPac AG11-HC (50 mm × 4 mm), an IonPac AS11-HC analytical column (250 mm × 4 mm), and an ED50 conductivity detector. All

experiments were performed at a flow rate of 1.0 mL min<sup>-1</sup> and with a 30 °C oven temperature. The samples were injected through a 0.22 mm filter before entering the IC system. The elution buffer was 24 mM of NaOH.

## ■ ASSOCIATED CONTENT

### 📄 Supporting Information

Experimental conditions for the analysis of stereoselectivity of mutants, the position of the adenine moiety of NAD in oxidoreductases (Figure S1 and Table S1), and HPLC chromatogram of lactate enantiomers (Figure S2). This material is available free of charge via the Internet at <http://pubs.acs.org>.

## ■ AUTHOR INFORMATION

### Corresponding Author

zhaozb@dicp.ac.cn

## ■ ACKNOWLEDGMENTS

We thank the National Natural Science Foundation of China (no. 20472084) and the National Basic Research and Development Program of China (no. 2012CB721103) for financial supports.

## ■ REFERENCES

- (1) Blank, L. M.; Ebert, B. E.; Buehler, K.; Bühler, B. *Antioxid. Redox Signal.* **2010**, *13*, 349–394.
- (2) Pollak, N.; Dolle, C.; Ziegler, M. *Biochem. J.* **2007**, *402*, 205–218.
- (3) (a) Houtkooper, R. H.; Cantó, C.; Wanders, R. J.; Auwerx, J. *Endocr. Rev.* **2010**, *31*, 194–223. (b) Ying, W. H. *Antioxid. Redox Signal.* **2008**, *10*, 179–206.
- (4) (a) Yang, H. Y.; Yang, T. L.; Baur, J. A.; Perez, E.; Matsui, T.; Carmona, J. J.; Lamming, D. W.; Souza-Pinto, N. C.; Bohr, V. A.; Rosenzweig, A.; Cabo, R.; Sauve, A. A.; Sinclair, D. A. *Cell* **2007**, *130*, 1095–1107. (b) Holm, A. K.; Blank, L. M.; Oldiges, M.; Schmid, A.; Solem, C.; Jensen, P. R.; Vemuri, G. N. *J. Biol. Chem.* **2010**, *285*, 17498–17506.
- (5) (a) Ruth, C.; Glieder, A. *ChemBioChem* **2010**, *11*, 761–765. (b) McLachlan, M. J.; Chockalingam, K.; Lai, K. C.; Zhao, H. M. *Angew. Chem., Int. Ed.* **2009**, *48*, 7783–7786.
- (6) Prescher, J. A.; Bertozzi, C. R. *Nat. Chem. Biol.* **2005**, *1*, 13–21.
- (7) (a) Miller, S. P.; Lunzer, M.; Dean, A. M. *Science* **2006**, *314*, 458–461. (b) Khattab, S. M. R.; Watanabe, S.; Saimura, M.; Kodaki, T. *Biochem. Biophys. Res. Commun.* **2011**, *404*, 634–637. (c) Khoury, G. A.; Fazelinia, H.; Chin, J. W.; Pantazes, R. J.; Cirino, P. C.; Maranas, C. D. *Protein Sci.* **2009**, *18*, 2125–2138.
- (8) Zorn, J. A.; Wells, J. A. *Nat. Chem. Biol.* **2010**, *6*, 179–188.
- (9) Stockwell, B. R. *Nature* **2004**, *432*, 846–854.
- (10) (a) Shah, K.; Liu, Y.; Deirmengian, C.; Shokat, K. M. *Proc. Natl. Acad. Sci. U.S.A.* **1997**, *94*, 3565–3570. (b) Kraybill, B. C.; Elkin, L. L.; Blethrow, J. D.; Morgan, D. O.; Shokat, K. M. *J. Am. Chem. Soc.* **2002**, *124*, 12118–12128. (c) Ubersax, J. A.; Woodbury, E. L.; Quang, P. N.; Paraz, M.; Blethrow, J. D.; Shah, K.; Shokat, K. M. *Nature* **2003**, *425*, 859–864.
- (11) (a) Abramova, T. V.; Vasileva, S. V.; Serpokrlyova, I. Y.; Kless, H.; Silnikov, V. N. *Bioorg. Med. Chem.* **2007**, *15*, 6549–6555. (b) Hou, S. H.; Liu, W. J.; Ji, D. B.; Wang, Q.; Zhao, Z. K. *Tetrahedron Lett.* **2011**, *52*, 5855–5857.
- (12) Chockalingam, K.; Chen, Z. L.; Katzenellenbogen, J. A.; Zhao, H. M. *Proc. Natl. Acad. Sci. U.S.A.* **2005**, *102*, 5691–5696.
- (13) Chang, G. G.; Tong, L. *Biochemistry* **2003**, *42*, 12721–12733.
- (14) (a) Bordoli, L.; Kiefer, F.; Arnold, K.; Benkert, P.; Battey, J.; Schwede, T. *Nat. Protoc.* **2009**, *4*, 1–13. (b) Schwede, T.; Kopp, J.; Guex, N.; Peitsch, M. C. *Nucleic Acids Res.* **2003**, *31*, 3381–3385.
- (15) Wang, J. X.; Zhang, S. F.; Tan, H. D.; Zhao, Z. K. *J. Microbiol. Methods* **2007**, *71*, 225–230.

- (16) Reetz, M. T.; Kahakeaw, D.; Lohmer, R. *ChemBioChem* **2008**, *9*, 1797–1804.
- (17) Mayer, K. M.; Arnold, F. H. *J. Biomol. Screen.* **2002**, *7*, 135–140.
- (18) Ellington, A. D.; Bull, J. J. *Science* **2005**, *310*, 454–455.
- (19) (a) Rossmann, M. G.; Moras, D.; Olsen, K. W. *Nature* **1974**, *250*, 194–198. (b) Bottoms, C. A.; Smith, P. E.; Tanner, J. J. *Protein Sci.* **2002**, *11*, 2125–2137.
- (20) Carugo, O.; Argos, P. *Proteins* **1997**, *28*, 10–28.
- (21) Kochhar, S.; Hottinger, H.; Chuard, N.; Taylor, P. G.; Atkinson, T.; Scawen, M. D.; Nicholls, D. J. *Eur. J. Biochem.* **1992**, *208*, 799–805.
- (22) Hall, M. D.; Banaszak, L. J. *J. Mol. Biol.* **1993**, *232*, 213–222.
- (23) Muramatsu, H.; Mihara, H.; Goto, M.; Miyahara, I.; Hirotsu, K.; Kurihara, T.; Esaki, N. *J. Biosci. Bioeng.* **2005**, *99*, 541–547.
- (24) (a) Haferkamp, I.; Schmitz-Esser, S.; Linka, N.; Urbany, C.; Collingro, A.; Wagner, M.; Horn, M.; Neuhaus, H. E. *Nature* **2004**, *432*, 622–625. (b) Todisco, S.; Agrimi, G.; Castegna, A.; Palmieri, F. *J. Biol. Chem.* **2006**, *281*, 1524–1531. (c) Palmieri, F.; Rieder, B.; Ventrella, A.; Blanco, E.; Do, P. T.; Nunes-Nesi, A.; Trauth, A. U.; Fiermonte, G.; Tjaden, J.; Agrimi, G.; Kirchberger, S.; Paradies, E.; Fernie, A. R.; Neuhaus, H. E. *J. Biol. Chem.* **2009**, *284*, 31249–31259.
- (25) Zhou, Y. J.; Wang, L.; Yang, F.; Lin, X. P.; Zhang, S. F.; Zhao, Z. K. *Appl. Environ. Microbiol.* **2011**, *77*, 6133–6140.
- (26) Yoshikawa, M.; Kato, T.; Takenish, T. *Tetrahedron Lett.* **1967**, *8*, 5065–5068.
- (27) Liu, R.; Visscher, J. *Nucleosides Nucleotides* **1994**, *13*, 1215–1216.
- (28) Wang, J. X.; Tan, H. D.; Zhao, Z. K. *Protein Expression Purif.* **2007**, *53*, 97–103.